CONTROL OF LASER RADIATION PARAMETERS

PACS numbers: 42.55.Lt; 42.60.Mi; 42.65.Sf
DOI: 10.1070/QE2011v041n05ABEH014517

Self-heterodyne detection of backscattered radiation in single-mode CO_2 lasers

V.M. Gordienko, A.N. Konovalov, V.A. Ul'yanov

***Abstract*. Self-heterodyning in dc-discharge-pumped single-mode CO_2 lasers is analysed theoretically and studied experimentally under strong and weak feedback conditions. Relations for the autodyne gain and modulation depth due to the effect of backscattered radiation with a Doppler-shifted frequency are obtained. Nonlinear distortions of the autodyne signal caused by a strong laser – target feedback are studied. It is shown that the autodyne detection of backscattered radiation in CO_2 lasers can be considered linear even in the case of strong laser beam distortions (nonlinear distortions below 5 %).**

Keywords: *autodyne gain, backscattered radiation, single-mode CO_2 laser*.

1. Introduction

Self-heterodyning, which is sometimes called the autodyne effect, consists in the modulation of initial laser radiation and pump current by laser radiation with a Doppler-shifted frequency backscattered into the laser cavity from an external moving object [1]. Self-heterodyning is distinguished by the following features: first, the scheme of detection of scattered radiation is monostatic and self-matched (which means that, in the case of diffusion scattering, matching of the scattered and initial laser radiation occurs automatically), and, second, the primary detector of the scattered radiation is the laser itself, which leads to a finite detection band and to a nonlinear dependence of the autodyne signal on the level of external action. At high backscattering coefficients, there exists a strong feedback accompanied by a complex nonlinear dynamics of laser radiation characteristics, including the appearance of chaos. The autodyne regime is of great practical importance and is used for solving such problems as measurement of speeds [1, 2], detection of small oscillations [3 – 5], measurement of distances [2, 6 – 8], and analysis of atmospheric gases [8 – 10]. For intracavity detection of reflected or scattered radiation, one uses semiconductor [2, 3, 6, 7, 11], solid-state [4, 12], and CO_2 [1, 8 – 10] lasers, as well as, recently, diode-pumped chip lasers [13] and fibre lasers [14].

The behaviour of the autodyne effect is studied experimentally and theoretically mainly for semiconductor lasers [2, 3, 6, 7, 11]. In works on CO_2 lasers [8 – 10] and in numerous studies on semiconductor lasers [4, 5, 8, 9, 14], this effect was described based on the introduction of a third mirror into the laser cavity in the stationary lasing approximation or on the use of the equation for laser radiation intensity in the approximation that the population inversion has some stationary value. In addition, backscattering is considered to be weak and cause small distortions. In the available literature, there are no data on the behaviour of the amplitude and spectral characteristics of autodyne signals in CO_2 lasers as functions of backscattered radiation characteristics. Single-mode CO_2 lasers with a high spatial quality of the beam and with a high average power are widely used in laser processing of materials and some medical technologies. The backscattered signal power depends on the radiation intensity and the type of material. It is obvious that self-heterodyning is promising for creating an optical feedback channel, which can be used for on-line monitoring and diagnostics of laser processing of materials.

Th aim of this work is to study theoretically and experimentally self-heterodyning in dc-discharge-pumped CO_2 lasers in a wide range of intensities of backscattered/reflected radiation.

2. Theory

We will describe the autodyne effect using the semiclassical two-level model of the active medium and the following assumptions: the luminescence line is homogeneously broadened; the field inside the cavity is approximated by a standing wave; lasing is single-mode and single-frequency; the laser belongs to the class B, which means that $\gamma_\perp \gg \gamma_\parallel \approx \gamma_c^{(0)}$, where $\gamma_c^{(0)}$ is the decay rate of the field in the cavity while $\gamma_\parallel$ and $\gamma_\perp$ are the longitudinal and transverse decay rates, respectively. Within these assumptions, we can obtain the following system of equations for slowly varying amplitudes [15, 16]:

$$\begin{aligned} \frac{\partial \boldsymbol{E}}{\partial t} &= -\gamma_c^{(0)}\boldsymbol{E} + \alpha(\omega_c)\boldsymbol{E}D, \\ \frac{\partial D}{\partial t} &= \gamma_\parallel(D_0 - D) - 4|\boldsymbol{E}|^2 D\mathrm{Re}\alpha(\omega_c), \end{aligned} \tag{1}$$

V.M. Gordienko Department of Physics and International Laser Centre, M.V. Lomonosov Moscow State University, Vorob'evy gory, 119991 Moscow, Russia; e-mail: gord@phys.msu.ru;
A.N. Konovalov, V.A. Ul'yanov Institute of Laser and Information Technologies, Russian Academy of Sciences, Pionerskaya ul. 2, 142190 Troitsk, Moscow region, Russia; e-mail: vaul595@mail.ru

Received 8 December 2010; revision received 10 February 2011
Kvantovaya Elektronika **41** (5) 433 – 440 (2011)
Translated by M.N. Basieva

$$\alpha(\omega_c) = \frac{|\xi|^2}{\gamma_\perp + i(\omega_0 - \omega_c)},$$

where $\boldsymbol{E}$ is the slowly varying amplitude of the field in the cavity (the total field is represented in the form $\boldsymbol{E} = \boldsymbol{E}(t) \times \exp(-i\omega_c t)$ and normalised so that the wave intensity in the cavity is $\hbar\omega_c|\boldsymbol{E}|^2/2$; ω_c is the optical cavity mode frequency; $D = U - G$ is the population inversion; U and G are the populations of the upper and lower laser levels; D_0 describes the laser pumping and is equal to the average population inversion that would appear in the absence of a field in the cavity; ξ is the coupling constant; and ω_0 is the central frequency of the gain line.

System (1) does not include an equation for polarisation because, for class-A and class-B lasers ($(\gamma_\perp \gg \gamma_\parallel, \gamma_c)$, polarisation has time to follow the field $\boldsymbol{E}$ and the inversion D. The equation for the field contains the following term describing the field decay in the cavity [17]:

$$\gamma_c^{(0)} = -\frac{c}{2L}\ln(r_1 r), \tag{2}$$

where r is the reflection coefficient of the output cavity mirror; r_1 is the effective reflection coefficient of the second mirror, which takes into account both the mirror reflectance and additional losses due to, for example, diffraction; and L is the cavity length.

The exponential decay of the field in the cavity with a rate described by expression (2) is obtained when we consider the field dynamics taking into account the reflection from the output mirror. The appearance of back-reflected/scattered radiation in the cavity can be described as reflection from an output mirror composed of the cavity mirror and an external object. In the general case of an external moving mirror, the problem of the dynamics of laser characteristics cannot be solved analytically, since the frequency of the time-delayed radiation reflected/scattered from an object differs from the frequency of radiation in the cavity due to both the Doppler effect and a change in the cavity frequency with time. Because of this, the literature mainly contains only limiting cases related to the steady-state lasing approximation, when the laser-level population dynamics is not taken into account [6–9]. The applicability of one or another approximation depends on the type of the used laser.

In this study, we consider the autodyne effect in single-mode CO_2 lasers as applied to the problems of detection of radiation backscattered from objects spaced from the laser at short distances, such that the change in the instantaneous frequency of the cavity mode for the time of the echo-signal delay can be neglected. In this case, the effect of the external object is reduced to a change in the reflection coefficient of the composed mirror. Let us find the condition at which this approximation is valid.

A change in the cavity mode frequency can be estimated from the relation that follows from the steady-state lasing condition in the presence of an external mirror [7]

$$2KL + a\sin(2KL_e) = 2\pi n, \tag{3}$$

where $n = 1, 2, 3, \ldots$; $K = \omega_c/c$ is the wave number; $a \equiv \beta(1 - r_{out}^2)/r_{out}$; r_{out} is the modulus of the field reflection coefficient of the output mirror; β is the coefficient of field back-reflection/scattering from an external object; and L_e is the distance from the output mirror to the object.

Relation (3) is obtained in the assumption that $a \ll 1$. Taking $K = K_0 + \Delta K = (\omega_0 + \Delta\omega)/c$, where K_0 is the wave number satisfying the lasing condition in the absence of a reflector ($2K_0L = 2\pi n$), we can derive

$$\Delta\omega = -\frac{ac}{2L}\cos\left(2L_e K_0 + \frac{2L_e\Delta\omega}{c}\right). \tag{4}$$

Differentiating (4) with respect to time, we find that the derivative $d\Delta\omega/dt$ changes with time and its maximum value is determined by the factor in front of sin(...). Let us estimate the parameters of the external reflector/scatterer at which the effects related to the echo-signal delay are weak. After differentiating (4), we can determine the maximum of the frequency shift derivative,

$$\frac{d\Delta\omega}{dt} \approx \frac{ac}{2L}\,2K_0\frac{dL_e}{dt} = \frac{ac}{2L}\,v_D, \tag{5}$$

where $v_D = 2K_0(dL_e/dt)$ is the Doppler frequency shift.

The frequency of the echo signal delayed by the time $\tau_e = 2L_e/c$ will be different from the laser frequency. The maximum of this frequency shift is

$$\frac{d\omega}{dt}\,\tau_e = \frac{ac}{2L}\,\frac{2L_e}{c}\,v_D. \tag{6}$$

The autodyne signal exhibits no distortions caused by the echo-signal delay if the frequency difference is much smaller than the Doppler frequency shift. This occurs under the condition

$$a\,\frac{L_e}{L} \ll 1. \tag{7}$$

For $L_e \leqslant L$, condition (7) is obviously valid. This cannot be said for detection at a large distance L_e. In this case, even weak scattering can cause autodyne signal distortions due to the echo-signal delay. The condition of the absence of such effects is determined by the backscattering coefficient

$$\beta^2 \ll \left(\frac{L}{L_e}\,\frac{r_{out}}{1 - r_{out}^2}\right)^2. \tag{8}$$

Even at $L_e = 10L$ and $r_{out}^2 = 0.9$, we have $\beta^2 \ll 0.9$, which is true for most applications.

Note that laser frequency fluctuations can also be caused by technical fluctuations, for example, by acoustic vibrations of the cavity mirrors [18]. Lasing stability is frequently characterised by the long-time and short-time stabilities. As a rule, the spectral bandwidth $\Delta\nu$ of single-frequency lasers is 10–100 kHz [17, 19], while the coherence length may exceed hundreds of meters. For self-heterodyning, the laser frequency fluctuations for the echo-signal delay time must be much smaller than the measured Doppler frequencies. At the object speeds of 1–10 m s^{-1} in the case of a single-mode single-frequency CO_2 laser ($v_D = 200$ kHz – 2 MHz), this factor is not so important at $L_e \sim L$ because the shift of the echo-signal frequency at such distances (much shorter than the coherence length) is considerably smaller than the laser bandwidth $\Delta\nu$ and the Doppler frequency shifts.

Thus, if condition (8) is fulfilled and the distance to the object is considerably smaller than the radiation coherence length, the external field entering the laser cavity is

determined only by the object itself and by the instantaneous value of the field in the cavity. In this case, we can introduce the concept of a composed output mirror as a Fabry–Perot interferometer formed by mirrors with reflection coefficients r_0 and β (coefficient of back-reflection/scattering from the external object). For this mirror, we can calculate the complex reflection coefficient which takes into account both the wave amplitude and phase,

$$r = r_0 + \tau_0\beta\,\frac{\exp(-\mathrm{i}KL_\mathrm{e})}{1 - r_0\beta\exp(-\mathrm{i}KL_\mathrm{e})} = r_0 + \mathrm{d}r, \tag{9}$$

where τ_0 is the laser mirror transmission coefficient.

The laser dynamics will also be described by Eqns (1), but, instead of the field decay rate $\gamma_\mathrm{c}^{(0)}$, we must use the complex parameter γ_c, which takes into account not only the decay of the field amplitude but also the change in the field phase upon reflection from the composed mirror,

$$\gamma_\mathrm{c} = -\frac{c}{2L}\ln(r_1 r) = \gamma_\mathrm{c}^{(0)}\left[1 + \frac{\ln(1 + \mathrm{d}r/r_0)}{\ln(r_1 r_0)}\right]$$

$$\equiv \gamma_\mathrm{c}^{(0)}(1 + p). \tag{10}$$

The equation for the field E in (1) can be easily transformed into the following equation for the value $I = EE^*$ (proportional to intensity):

$$\frac{\mathrm{d}I}{\mathrm{d}t} = E\,\frac{\mathrm{d}E^*}{\mathrm{d}t} + E^*\frac{\mathrm{d}E}{\mathrm{d}t} = -2I\{\mathrm{Re}\gamma_\mathrm{c}(t) - D\mathrm{Re}[\alpha(\omega_\mathrm{c})]\}. \tag{11}$$

For more correct description of the self-heterodyning process, we should use the rate equations for the active medium. To describe the amplification of radiation injected into a laser, we used a model developed in [15], which separately takes into account the dynamics of populations of the upper (U) and lower (G) laser levels. Introducing the dimensionless time $\tau = t\gamma_\mathrm{c}^{(0)}$, normalising the variables U and G to U_0 (stationary U in the absence of lasing), and introducing the parameter $C = U_0\mathrm{Re}(\alpha)/\gamma_\mathrm{c}^{(0)}$, which characterises pumping, we obtain for this model the system of equations

$$\frac{\mathrm{d}I}{\mathrm{d}\tau} = -2I[1 - \mathrm{Re}p(t) - C(U - G)],$$

$$\frac{\mathrm{d}U}{\mathrm{d}\tau} = \bar{\gamma}_\parallel(1 - U) - (U - G)I, \tag{12}$$

$$\frac{\mathrm{d}G}{\mathrm{d}\tau} = \bar{\gamma}_1(G_0 - G) + \bar{\gamma}_\parallel U + (U - G)I,$$

where $\bar{\gamma}_\parallel = \gamma_\parallel/\gamma_\mathrm{c}^{(0)}$; $\bar{\gamma}_1 = \gamma_1/\gamma_\mathrm{c}^{(0)}$, and γ_1 is the relaxation rate of the lower laser level.

The first term in Eqn (12) describes the relaxation of populations to the stationary value G_0, the second term corresponds to the spontaneous transition from the upper to the lower laser level, and the third term describes the transition stimulated by the field in the cavity.

Consider the case of a weak feedback, when $\mathrm{Re}p \ll 1$. The weak action of the reflected radiation slightly disturbs stationary lasing. We will write the expressions for the laser radiation intensity and the population inversion in the form

$$I = I_0 + i(\tau),$$

$$G = G^{(0)} + g(\tau), \tag{13}$$

$$U = U^{(0)} + u(\tau),$$

where $I_0 = \bar{\gamma}_\parallel[C(1 - G^{(0)}) - 1]$, $U^{(0)} = 1/C + G^{(0)}$, and $G^{(0)} = \bar{\gamma}_\parallel/\gamma_1 + G_0$ are the stationary intensities and populations of the upper and lower levels in the absence of a target; $i(\tau)$, $u(\tau)$, and $g(\tau)$ are the small deviations of the corresponding parameters from their values in the case of stationary lasing.

Let us linearise the system of equations (12) by substituting (13) and taking into account only the first order of smallness for i, u, and g,

$$\frac{\mathrm{d}i}{\mathrm{d}\tau} = -2I_0Cu - 2I_0CI + 2I_0\mathrm{Re}p(t),$$

$$\frac{\mathrm{d}u}{\mathrm{d}\tau} = -\frac{i}{C} - u(\bar{\gamma}_\parallel + I_0) - II_0, \tag{14}$$

$$\frac{\mathrm{d}I}{\mathrm{d}\tau} = \frac{i}{C} + u(\bar{\gamma}_\parallel + I_0) - I(I_0 + \bar{\gamma}_1).$$

As is known, a linear system can be solved for complex values. Then, for a weak feedback, from (9) and (10) we obtain

$$\mathrm{d}r = \tau_0\beta\exp(-\mathrm{i}KL_\mathrm{e}),$$

$$p = \frac{\ln(1 + \mathrm{d}r/r_0)}{\ln(r_1 r_0)} \approx \frac{\mathrm{d}r}{r_0\ln(r_1 r_0)} = \frac{\tau_0\beta\exp(-v_\mathrm{D}t)}{r_0\ln(r_1 r_0)}. \tag{15}$$

In the case of uniform motion ($L_\mathrm{e} = L_0 + Vt$) of an object with the constant scattering coefficient β, we have

$$p(\tau) = \frac{\tau_0\beta}{r_0\ln(r_1 r_0)}\exp(\mathrm{i}\Omega\tau) \equiv \kappa\beta\exp(\mathrm{i}\Omega\tau), \tag{16}$$

where $\Omega = 2K_0V/\gamma_\mathrm{c}^{(0)}$ is the Doppler frequency shift normalised to $\gamma_\mathrm{c}^{(0)}$.

The solution of linear system (14) has the form $i = i_0\exp(\mathrm{i}\Omega\tau)$, $u = u_0\exp(\mathrm{i}\Omega\tau)$. For the variable intensity component, we find

$$|i_0|^2 = (2I_0\kappa\beta)^2\left|\mathrm{i}\Omega + 2I_0\,\frac{1 - F(\Omega)}{\mathrm{i}\Omega + \bar{\gamma}_\parallel + I_0 - I_0F(\Omega)}\right|^{-2}$$

$$\equiv 4I_0^2\beta^2H(\Omega), \tag{17}$$

where

$$F(\Omega) = -\frac{\mathrm{i}\Omega}{\mathrm{i}\Omega + \bar{\gamma}_\parallel}.$$

Thus, the autodyne signal power is proportional to the backscattered beam power $I_0\beta^2$. The introduced function $H(\Omega)$ characterises the enhancement of the autodyne effect and is equal to the power ratio of the autodyne signal and the equivalent heterodyne signal obtained in the case of mixing the reference radiation, whose intensity is equal to the laser output intensity I_0T ($T = \tau_0^2$), and the scattered radiation with the intensity $I_0\beta^2$. Indeed, the autodyne

signal power at the laser exit is $P_a = |i_0|^2 T^2$, while the equivalent heterodyne signal power is $P_g = 4T^2 I_0^2 \beta^2$. The modulation depth due to the autodyne effect is

$$M \equiv \frac{|i_0|}{I_0} = 2\sqrt{H(\Omega)\beta^2}. \tag{18}$$

Figure 1 shows the autodyne gain dependences $H(v_D)$ calculated by formula (17) corresponding to system (14). The laser parameters were selected by the best coincidence of the experimental and calculated amplitude–frequency characteristics (see below). Figure 2 presents the dependence of the autodyne gain at the resonance maximum ($\Omega = \Omega_0$) on the parameter C (on the output power).

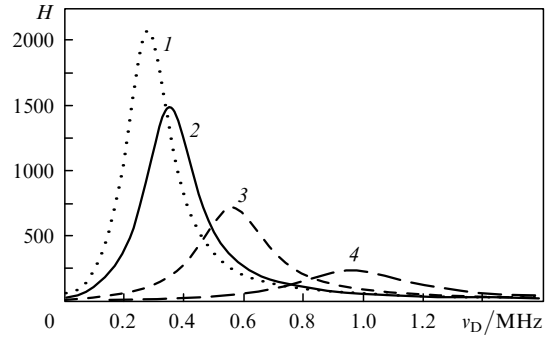

Figure 1. Amplitude–frequency characteristic of autodyne detection for a cw single-mode CO_2 laser at the output powers $P = 1$ W ($C = 1.8$) (*1*), 1.5 W ($C = 2.05$) (*2*), 3.5 W ($C = 3.07$) (*3*), and 10 W ($C = 6.4$) (*4*) for the calculation parameters $\gamma_c^{(0)} = 10^7$ s^{-1}, $\bar{\gamma}_\parallel = 0.01$, $\gamma_\parallel = 0.024$, $\bar{\gamma}_1 = 0.18$, $G_0 = 0.088$, $r_0 = 0.964$, and $r_1 = 0.97$.

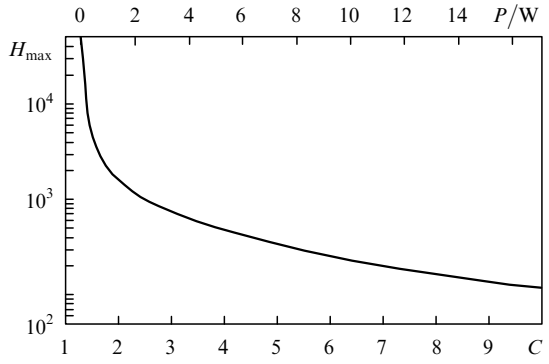

Figure 2. Dependence of the autodyne gain at the resonance frequency on the pump parameter. The calculation parameters are the same as in Fig. 1.

Above, we assumed that the scattering object is a uniformly moving mirror with the intensity reflection coefficient β^2. In the case of a complex scattering object, the time function $p(t)$, which describes the feedback, can be expanded into spectral components, and the general solution of linear system (14) for distortion of lasing at a weak feedback can be represented as the sum of solutions for each of the separate components. Thus, the autodyne signal spectrum at a weak feedback will represent the spectrum of the scattered radiation power multiplied by the autodyne gain dependence $H(\Omega)$. The obtained amplitude–frequency characteristic $H(\Omega)$ (17) for class-B lasers has a resonance shape due to the occurrence of relaxation oscillations.

At rather high backscattering coefficients, the above consideration cannot be used. In the general case, the variable component of the laser radiation intensity is not linear according to the Doppler function $\beta \exp(iv_D t)$, which characterises scattering by a moving object. Some features of this regime can be analysed without solving system (12) directly. The autodyne signal formation can be conventionally divided into two processes: the laser beam reflection from the external mirror and the amplification of the beat signal between the initial and the frequency-shifted reflected waves in the laser. For these processes, we also can separate two mechanisms of formation of the nonlinear autodyne signal (the appearance of additional harmonics along with the main harmonic at the Doppler frequency Ω): the multiple reflection of the amplified wave from the external object, which leads to the formation of frequencies divisible to Ω in the autodyne signal, and the proper nonlinear amplification of the signal in the laser.

We will characterise the autodyne signal by a nonlinear parameter determined as the ratio of the autodyne signal power P_2 at the doubled Doppler frequency 2Ω to the power P_1 at the Doppler frequency Ω,

$$\eta = P_2/P_1. \tag{19}$$

Since the autodyne signal depends on the Doppler frequency shift Ω, the parameter η also depends on Ω. The nonlinearity of the first process is maximum when $\Omega = \Omega_0/2$ because the second harmonic coincides with the autodyne gain maximum. The nonlinearity of the second process is maximum at $\Omega = \Omega_0$. Thus, the frequency dependence of the nonlinearity parameter also has a resonance shape, but this resonance is wider than the resonance of the amplitude–frequency characteristic. Figure 3 shows the dependence of P_2/P_1 on v_D obtained by numerically solving the system of equations (12).

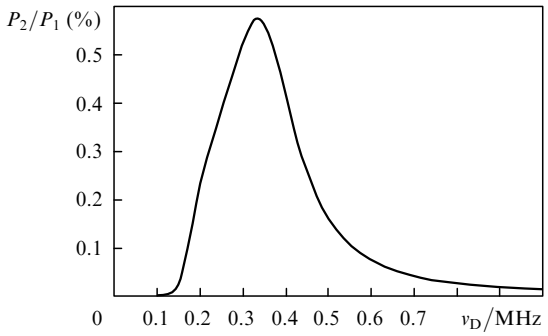

Figure 3. Dependence of the autodyne signal nonlinearity parameter on the Doppler frequency shift at $C = 2.05$. The calculation parameters are the same as in Fig. 1.

Figures 4 and 5 present the dependences of the radiation modulation depth M and the nonlinearity coefficient η on the backscattering coefficient β^2 at $\Omega = \Omega_0$, which are also found by numerically solving the system of laser equations (12). As expected, the dependence of the modulation depth on β^2 in the log-log scale is linear for small values [see formula (18)]. At $\beta^2 > 10^{-3}$, the dependence becomes noticeably nonlinear. At such backscattering coefficients, the nonlinear distortion is of the order of several percents. It is convenient to represent the obtained dependences in the

form of the dependence of the nonlinearity parameter on the modulation depth (Fig. 6). One can see that nonlinear distortions become significant ($\eta > 5\,\%$) at $M > 0.7$. This indicates that the autodyne detection of backscattered radiation in CO_2 lasers can be considered linear with an accuracy better than 5 % even at strong distortions of laser radiation leading to modulation with an amplitude close to 0.5.

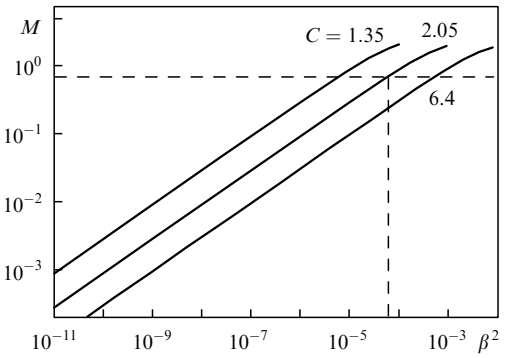

Figure 4. Dependence of the autodyne signal modulation depth on the backscattering coefficient. The calculation parameters are the same as in Fig. 1.

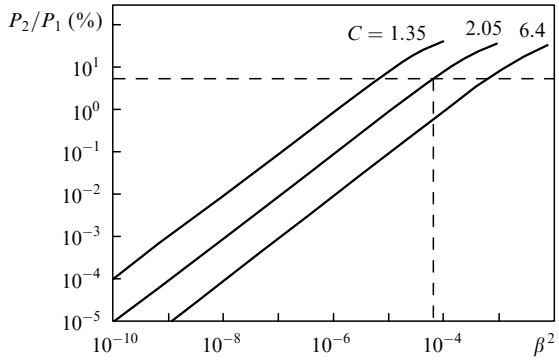

Figure 5. Dependence of the autodyne signal nonlinearity parameter on the backscattering coefficient. The calculation parameters are the same as in Fig. 1.

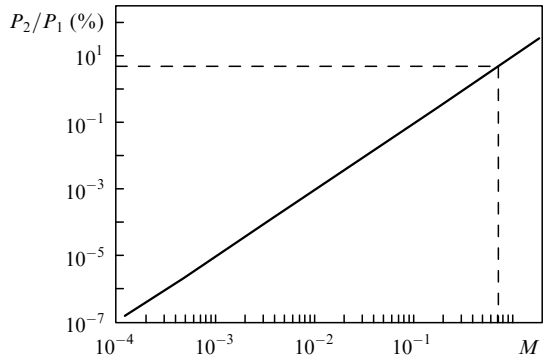

Figure 6. Dependence of the autodyne signal nonlinearity parameter on the modulation depth of the laser radiation power. The calculation parameters are the same as in Fig. 1.

3. Experiment

The scheme of the experimental setup used to study the autodyne detection in a dc-discharge-pumped single-mode CO_2 laser with a power of 2 W is shown in Fig. 7. In this scheme, we realise three types of detection of scattered radiation: direct detection, autodyne detection, and heterodyning. A part of laser radiation is sent to a cooled HgCdTe IR detector using beam splitting wedges (*4*) and (*11*), mirror (*9*), and focusing lens (12). This channel [(*4*)–(*9*)–(*11*)] was used both to detect the laser power modulation (autodyne signal) and to form a reference beam and observe the heterodyne signal. The backscattered radiation was also sent to photodetector (*14*) using wedge (*5*) and mirrors (*8*) and (*3*). The optical channels (*4*)–(*9*)–(*11*) and (*5*)–(*8*)–(*3*)–(*11*) were combined so that the photodetector received the difference-frequency heterodyne signal formed due to scattering from rotating disk (*7*). When the channel (*4*)–(*9*)–(*11*) was closed, the photodetector recorded the backscattered radiation, and, with the closed channel (*5*)–(*8*)–(*3*)–(*11*), the photodetector recorded the autodyne signal in the form of laser power beating.

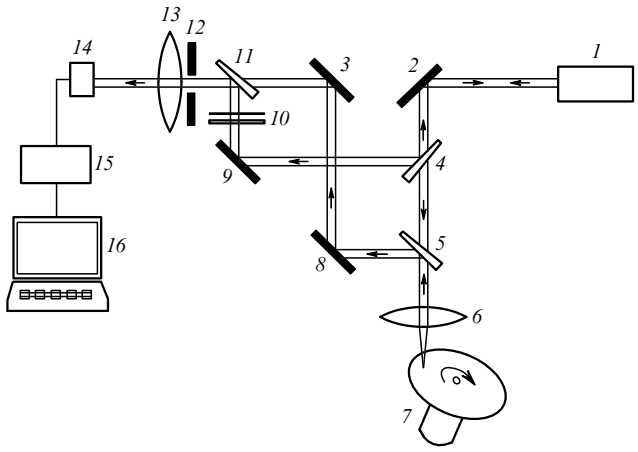

Figure 7. Scheme of the setup for investigating autodyne detection in a CO_2 laser: (*1*) single-mode CO_2 laser; (*2*, *3*, *8*, *9*) mirrors; (*4*, *5*, *11*) beam-splitting wedges; (*6*, *13*) lenses; (*7*) rotating disk (disk with blades or plexiglas); (*10*) attenuators; (*12*) aperture; (*14*) cooled HgCdTe photodetector; (*15*) analog-to-digital converter; (*16*) computer.

For recording and subsequent processing, the signal from the photodetector was amplified and sent to analog-to-digital converter (*15*) connected to computer (*16*). To obtain the autodyne signal at a particular frequency, we used rotating disc (*7*). The radiation scatters from the disc, whose frequency is shifted due to the Doppler effect, returns to the laser cavity, and causes the modulation of the laser radiation power. The Doppler frequency changes with changing the disc rotation rate. To measure the amplitude–frequency characteristic of the autodyne detection, we measured the signal power at different Doppler frequency shifts. The measurement results are shown in Fig. 8. The experimental amplitude–frequency characteristic well agrees with model (*12*), which takes into account the population of the lower laser level.

The modulation depth in the sensitivity maximum was $\sim 5\,\%$ at the backscattering coefficient $\beta^2 \sim (2-5) \times 10^{-5}$.

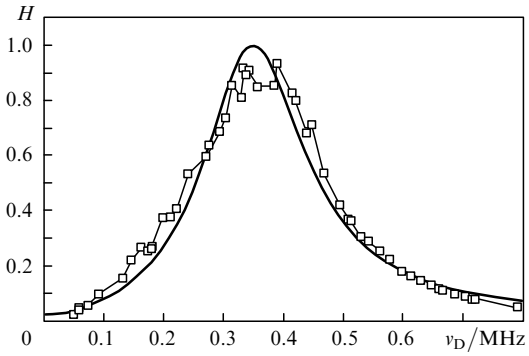

Figure 8. Amplitude–frequency characteristic of autodyne detection normalised to the autodyne gain maximum for a cw single-mode CO_2 laser. The points are the experimental data at an output power of 1.5 W. The thick curve is calculated by formula (19) taking into account the population of the lower level. The calculation parameters are the same as in Fig. 1.

The coefficient β^2 was determined by measuring the scattered radiation power and by direct detection taking into account the attenuation of radiation by beam-splitting wedges and attenuators (*10*). In front of the detecting face of photodetector (*14*), we placed aperture (*12*) to record the scattered radiation falling into the laser beam aperture. From the measured parameters, we have

$$H_{\text{eff}} = \left(\frac{M}{2}\right)^2 \frac{1}{\beta^2} \sim 10 - 30. \qquad (20)$$

This value is smaller than that calculated by formula (18). This occurs because the laser and backscattered radiations in theoretical calculations were considered as plane waves without taking into account the so-called front-matching factor (this term is used in optical heterodyning to characterise the efficiency of mixing of reference and signal beams [20]).

We studied the possibility of finding the real scattered radiation spectrum from the autodyne signal spectrum. To obtain the scattered signal in a wide spectral band, we used a plexiglas target placed in the lens focus. The plexiglas target was uniformly moved perpendicular to the laser beam with a velocity of 3–5 mm s^{-1}. This movement causes no noticeable Doppler frequency shift because the velocity vector has no component coaxial with the laser beam. In this case, the scattered radiation spectrum is determined by the laser-induced mass transfer in the area of interaction of the laser beam (intensity $\sim 10^3$ W cm^{-2}) with plexiglas. Figure 9 presents the power spectra of the autodyne and heterodyne signals appeared in the case of such action to plexiglas. Figure 10 shows the spectrum obtained by dividing the autodyne signal spectrum to the amplitude–frequency characteristic shown in Fig. 8. As seen, the heterodyne signal spectrum well coincides with the spectrum obtained by this procedure, which experimentally proves the conclusion based on the above analysis that the autodyne signal spectrum is a product of the spectra of the scattered radiation and the resonance amplitude–frequency characteristic.

To study the autodyne effect at high feedback coefficients, we used as a scatterer a rotating disc with blades whose surfaces at some instants were perpendicular to the laser beam, which provided the coefficient $\beta^2 \approx 10^{-2}$. A

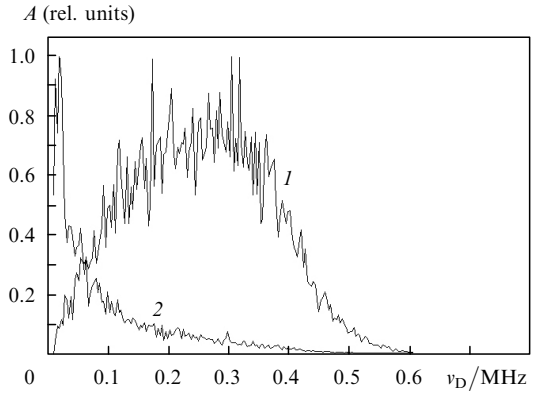

Figure 9. Power spectra of the heterodyne (*1*) and autodyne (*2*) signals obtained upon melting of plexiglas by radiation of a CO_2 laser with a power of 1.5 W.

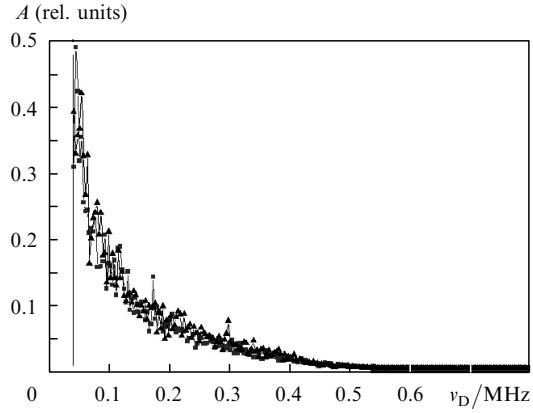

Figure 10. Power spectra of the heterodyne signal (▲) and of the autodyne signal divided by the amplitude–frequency characteristic of autodyne detection (■) obtained upon melting of plexiglas by radiation of a CO_2 laser with a power of 1.5 W.

system of laser beam attenuators (*10*) allowed us to change the backscattering coefficient within the range from $5 \times 10^{-4} - 10^{-2}$ to 10^{-2}. At the instant when a blade passed through the laser beam, the autodyne signal appeared at a Doppler frequency depending on the disk rotation rate. Figure 11 shows the time sweep of this autodyne signal. One can see that the signal has a periodic character, but its

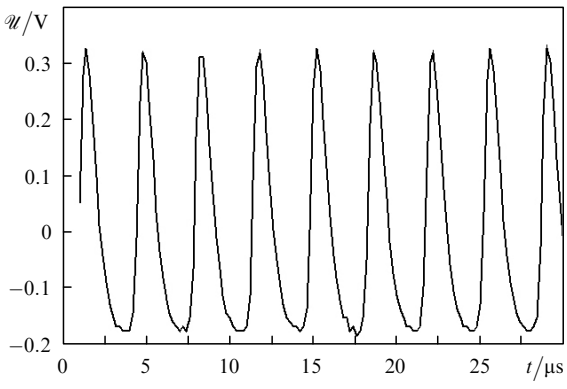

Figure 11. Time sweep of the autodyne signal in the strong feedback regime at $v_D = 0.25$ MHz, $P_2/P_1 = 0.25$, $\beta^2 \sim 10^{-3}$.

spectrum reveals a nonlinearity in the form of additional harmonics. The modulation depth M is 1.4.

In the example of the autodyne signal shown in Fig. 11, the ratio of its power at the doubled frequency to the power at the main frequency is $P_2/P_1 = 0.25$. Figure 12 presents the dependence of P_2/P_1 on v_D obtained experimentally at the backscattering coefficient $\beta^2 \sim 5 \times 10^{-4}$. The experiment showed that the autodyne signal with a high accuracy ($P_2/P_1 \leqslant 5\,\%$) can be considered linear with respect to the backscattering coefficient at $\beta^2 \leqslant 2 \times 10^{-3}$, which well agrees with the theoretical results. This resistance of CO_2 lasers to the action of back-reflected radiation opens the possibility of using the autodyne effect in the problems of remote and on-line monitoring of destructive action of laser radiation on condensed matter.

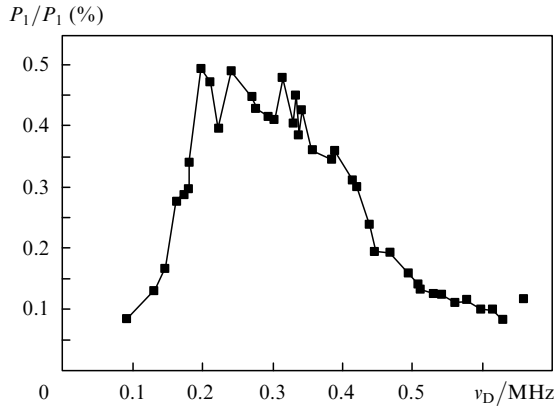

Figure 12. Experimental dependence of the autodyne signal nonlinearity parameter on the Doppler frequency shift at the backscattering coefficient $\beta^2 \sim 5 \times 10^{-4}$.

Based on this approach, we develop a method of diagnostics of the ablation of biological tissues in the process of laser surgery [21]. It was found that, when a CO_2 laser irradiates a biological tissue, its output radiation becomes modulated with a depth of 10 % – 15 %. According to the theoretical analysis performed above, this modulation depth at the pump parameter $C > 2$ corresponds to the nonlinearity parameter $\eta < 0.5\,\%$ (Figs 4 and 6). This points to the existence of a weak feedback and an unambiguous relation between the autodyne signal and the backscattered radiation carrying information on the mass transfer in the region of laser ablation of the biological tissue.

The considered approach can also be efficiently used in laser processing of materials, including metals, when reflection coefficients are high. It is known [18, 22] that, depending on the intensity of the 10-μm radiation and the metal type, the portion A_a of radiation absorbed by a metal varies in a wide range, beginning from 0.1 to values close to unity ($A_a \geqslant 0.9$) in the regime of deep (dagger-like) channeling. Then, assuming that the rest of the power is spent on backscattering into the solid angle 2π, we find that the power of radiation backscattered into the laser cavity is $0.1(d/f)^2/8$ (where d is the laser beam diameter and f is the focal length of the lens). At $f = 25$ cm and $d = 2$ cm, we have $\beta \approx 8 \times 10^{-5}$. At this backscattering coefficient, according to the above analysis (Fig. 5), the nonlinearity parameter at $C > 5$ (for technological CO_2 lasers, $C = 3 - 4$ [17]) will be several percents. A weak feedback will be also realised in the problems of remote ($f = 10 - 100$ m) destructive irradiation of materials by CO_2 lasers, since the value $(d/f)^2$ is small and, according to (8), the effect of the echo-signal time delay is insignificant. Thus, even in processing of metals by high-power laser radiation, the interaction of radiation with metal under particular conditions can be diagnosed by autodyne signals.

4. Conclusions

The autodyne effect in dc-discharge-pumped single-mode CO_2 lasers is analysed theoretically and studied experimentally in a wide range of backscattered/reflected radiation intensities ($\beta^2 = 10^{-11} - 10^{-2}2$). It is established that, at the distance to the scattering object $L_e \ll L[\beta(1 - r_{out}^2)/r_{out}]^{-1}$, the autodyne process in CO_2 lasers is linear ($\eta < 5\,\%$, weak feedback) even if the distortion of the laser radiation is strong and causes modulation with an amplitude close to 0.5. It is shown that, in these regimes, the backscattered radiation spectrum can be reconstructed from the spectrum of the output beat signal. This allows one to obtain information on the external moving object, for example, on its reflection/scattering coefficients and velocity, and to monitor the mass removal in the on-line mode upon laser ablation of biological tissues and laser processing of materials. Due to some specific features of CO_2 lasers (cavity length $L > 1$ m, insensitivity to the backward signal value), self-heterodyning can also be efficiently used for monitoring the remote destructive action of laser radiation on materials at distances of 10 – 100 m.

Acknowledgements. The authors thank V.Ya. Panchenko, A.K. Dmitriev, and V.N. Kortunov for useful and fruitful discussions of the results of this study. This work was supported by the Russian Foundation for Basic Research (Grant No. 08-08-00287).

References

1. Choi J.W., Yu M.J., Kopica M. *Proc. Soc. Photo-Opt. Instrum.*, **5240**, 230 (2004).
2. Giuliani G., Norgia M., Donati S., Bosch T. *J. Opt. A: Pure Appl. Opt.*, **4**, S283 (2002).
3. Usanov D.A., Skripal' A.V., Vagarin V.A. *Prib. Tekh. Eksp.*, **6**, 162 (1994).
4. Mak A.A., Orlov O.A., Ustyugov V.I. *Proc. SPIE Int. Soc. Opt. Eng.*, **1121**, 485 (1989).
5. Scalise L., Paone N. *Opt. Lasers Eng.*, **38**, 173 (2002).
6. Usanov D.A., Skripal' A.V., Avdeev K.S. *Pis'ma Zh. Tekh. Fiz.*, **33**, 72 (2007).
7. De Groot P.J., Galatin G.M., Macomber S.H. *Appl. Opt.*, **27**, 4475 (1988).
8. Koganov G.A., Shuker R., Gordov E.P. *Appl. Opt.*, **44**, 3105 (2005).
9. Koganov G.A., Shuker R., Gordov E.P. *Appl. Opt.*, **41**, 7087 (2002).
10. Gordov E.P., Khmelnitskii G.S., Fasliev A.Z. *Proc. SPIE Int. Soc. Opt. Eng.*, **2773**, 160 (1995).
11. Acket G.A., Lenstra D., den Boef A.J., Verbeek B.H. *IEEE J. Quantum Electron.*, **20**, 1163 (1984).
12. Burakov S.D., Godlevskii A.P., Ostanin S.A. *Opt. Atmos.*, (5), 547 (1990).
13. Ko J., Ohtomo T., Abe K., Otsuka K. *Int. J. Modern Phys.*, **15**, 3369 (2001).
14. Laroche M., Bartolacci C., et al. *Opt. Lett.*, **33**, 2746 (2008).
15. Laudon R., Harris M. *Phys. Rev. A*, **48**, 681 (1993).

16. Haken H. *Laser Light Dynamics* (Amsterdam: North-Holland, 1985).
17. Svelto O. *Principles of Lasers* (New York: Springer-Verlag, 2004).
18. Panchenko V.Ya. *Glubokoe kanalirovanie i filamentatsiya moshchnogo lasernogo izlucheniya v veshchestve* (Deep Channeling and Filamentation of High-Power Laser Radiation in Matter) (Moscow: Interkontakt Nauka, 2009).
19. Kravtsov N.V., Nanii O.E. *Kvantovaya Elektron.*, **20** (4), 322 (1993) [*Quantum Electron.*, **23** (4), 272 (1993)].
20. Protopopov V.V., Ustinov N.D. *Lazernoe geterodinirovanie* (Laser Heterodyning) (Moscow: Nauka, 1985).
21. Varev G.A., Geinits A.V., Dmitriev A.K., Konovalov A.N., Kortunov V.N., Panchenko V.Ya., Reshetov I.V., Ul'yanov V.A. *Al'manakh Klin. Med.*, XVII (part 2), 164 (2008).
22. Prokhorov A.M., Konov V.I., Ursu I., Mikheilesku I.N. *Vzaimodeistvie lazernogo izlucheniya s metallami* (Interaction of Laser Radiation with Metals) (Moscow: Nauka, 1988).